# EXPERIMENTAL RECONSTRUCTION OF SOURCE 4D PHASE SPACE WITHOUT PRIOR KNOWLEDGE OF TRANSFER MATRIX

C. Zhang*, E. Echeverria, A. Flint, C. Pennington,
I. Bazarov, A. Bartnik, J. Maxson, Cornell University (CLASSE), Ithaca, NY, United States
C. Pierce, University of Chicago, Chicago, IL, United States
A. Galdi, University of Salerno, Fisciano, Italy
W. Li, Brookhaven National Laboratory, Upton, NY, United States

*Abstract*

We use the PHOEBE test beamline at Cornell to experimentally demonstrate a simple method for reconstructing the transverse 4D phase space of an electron beam at the source from downstream aperture scans of the beam. This method does not rely on detailed knowledge of the beamline transport, besides assuming that linearity and symplecticity are satisfied. We apply this method to measure the source 4D phase space of electrons emitted from a spatially-structured alkali-antimonide cathode with periodic quantum efficiency modulations. The reconstructed 4D phase space is checked for fidelity, and we observe that the source spatial distribution matches the spatial structure of the cathode, and the source momentum distribution produces a mean transverse energy that is consistent with 4D beam emittance measurements.

## INTRODUCTION

Understanding the physics of photoemission is important for engineering photocathodes that produce high-quality beams. However, much of the experimental work currently done in accelerators only focuses on ensemble beam quantities such as quantum efficiency (QE) and mean transverse energy (MTE) [1–3], instead of probing the full position and momentum distribution of the emitted electrons at the source. A method for measuring the phase space of the beam at the source, in particular, would provide insight into the local correlations between momentum and position induced by surface deformities (physical and chemical) at the high surface fields [4, 5] necessary for accelerator applications.

In this paper, we demonstrate a method where 4D transverse phase space measurements performed with a downstream aperture scan diagnostic can be used to reconstruct the 4D transverse phase space at the source. The reconstruction relies on experimentally determining the transfer matrix by measuring the beam moments, the centroids and covariances, at the aperture scan diagnostic and their dependence on experimentally accessible beam moments at the source, which is the beam position centroid in our setup. Once the transfer matrix is known, the source phase space can be calculated by applying the inverse transfer matrix to a measured downstream phase space.

We first discuss the theory behind this source reconstruction method, our experimental setup, and then discuss the practical implementation of this method for a spatially structured photocathode.

* cz266@cornell.edu

## 4D RECONSTRUCTION THEORY

A linear transfer matrix, **M**, is often a good approximation for relating the source position and momentum of a particle to its final position and momentum downstream near the design trajectory of a beamline. Here, we only consider the transverse positions and momentums $\{x, p_x, y, p_y\}$, but many of our results can be generalized to 6D provided a means to measure some of the longitudinal transfer matrix elements.

In principle, the elements of the transfer matrix between the source and the downstream beamline diagnostic can be measured by linearly fitting the final position and momentum of a particle measured at the beamline diagnostic to its source position and momentum. In practice, instead of measuring individual particle positions and momentums, we measure the beam centroid in 4D phase space since it transforms with the transfer matrix like a single particle. In addition, we often only have control over the source position centroid. In the case of a photocathode, this can be inferred from the position of the laser spot driving photoemission. As a result, we cannot directly measure the entire 4D transfer matrix, but we will shortly discuss additional constraints derived from the symplectic condition and beam covariances that will yield the full 4D transfer matrix.

For each laser position, the 4D phase space of the beam is measured, and the beam centroid is calculated. For phase space centroids $(x_1, p_{x,1}, y_1, p_{y,1})$ and $(x_2, p_{x,2}, y_2, p_{y,2})$ measured when the laser is at positions $(y_L, 0)$ and $(x_L, 0)$, respectively, we can directly measure the first and third columns of the transfer matrix,

$$\begin{pmatrix} m_{11} & m_{13} \\ m_{21} & m_{23} \\ m_{31} & m_{33} \\ m_{41} & m_{43} \end{pmatrix} = \begin{pmatrix} x_2/x_L & x_1/y_L \\ p_{x,2}/x_L & p_{x,1}/y_L \\ y_2/x_L & y_1/y_L \\ p_{y,2}/x_L & p_{y,1}/y_L \end{pmatrix}. \quad (1)$$

For convenience, we refer to this as the partial transfer matrix. In practice, the partial transfer matrix will be determined by linearly fitting the measured phase space centroids to the measured laser positions.

With the partial transfer matrix and a few additional assumptions, we can solve for the full 4D transfer matrix. A system of 5 independent non-linear equations can be obtained from the symplectic condition, $\mathbf{M}\Omega\mathbf{M}^T = \Omega$, where

$\Omega$ is,

$$\Omega = \begin{pmatrix} 0 & 1 & 0 & 0 \\ -1 & 0 & 0 & 0 \\ 0 & 0 & 0 & 1 \\ 0 & 0 & -1 & 0 \end{pmatrix}.$$

In addition, we can also consider the evolution of the beam covariance matrix in the beamline, which is given by $\mathbf{M}^{-1}\Sigma_f(\mathbf{M}^{-1})^T = \Sigma_i$, where $\Sigma_f$ and $\Sigma_i$ are the measured downstream and the source beam covariance matrices, respectively. The elements of the beam covariance matrices are defined as $\Sigma_{ij} = \langle v_i v_j \rangle$, for $v = \{x, p_x, y, p_y\}$.

For a typical disordered and polycrystalline photocathode, we assume that the position and momentum are independent. Or, in other words, the source position-momentum correlation is zero. This yields another 4 independent non-linear equations, $\langle xp_x \rangle_i = \langle xp_y \rangle_i = \langle yp_x \rangle_i = \langle yp_y \rangle_i = 0$, which is related to the measured beam covariances and transfer matrix by $\mathbf{M}^{-1}\Sigma_f(\mathbf{M}^{-1})^T = \Sigma_i$.

As a result, we have a total of 9 independent non-linear equations constraining the remaining 8 unknown transfer matrix elements, making this an overdetermined system of equations. We apply the Gauss-Newton method to numerically find a best-fit solution, which yields the full transfer matrix. The full transfer matrix can then be inverted and applied to a measured 4D phase space to reconstruct the entire 4D phase space at the source.

## EXPERIMENTAL DEMONSTRATION

To check the fidelity of the 4D source phase space reconstruction, we used a micro-patterned alkali-antimonide cathode in our beamline. The cathode consisted of a $Si/SiO_2$ substrate with a layer of copper deposited on top with a periodic lattice of holes that exposed the underlying $Si/SiO_2$ substrate. A thin film of Na-K-Sb was then grown on top of the copper layer using physical vapor deposition. In our growth conditions, the QE of the Na-K-Sb film grown on the copper is larger than that grown on $Si/SiO_2$; therefore periodically modulating the QE across the cathode when photoemission is driven at 405 nm.

The beamline used for demonstrating this method consists of a DC gun biased at 15 kV, which accelerates the beam, and the beam is then focused by a solenoid onto a circular aperture with a diameter of 30 μm. After the aperture, the transmitted beam traveled through a ~0.5 m drift section until it reached the detector. The detector consisted of a microchannel plate, which multiplied electrons and accelerated them onto a YAG scintillator screen imaged by a sCMOS camera. At the aperture, the 4D phase space of the beam is measured with an aperture scan [6].

For measuring the partial transfer matrix, we use a small laser spot size positioned within uniform regions of the cathode, such that the laser spot does not significantly overlap with the patterned fiducial markers. The 4D phase space of the beam is measured for 8 laser positions within a 200 μm by 200 μm region. We project the measured 4D phase space into 2D phase spaces and fit them with a 2D supergaussian, which then supplies the beam centroids and covariances required to solve for the full 4D transfer matrix. We then switch to a larger laser spot that covers the fiducial markers, measure the 4D phase space of the resulting beam, and reconstruct the source 4D phase space using the solved 4D transfer matrix.

## EXPERIMENTAL RESULTS

In Fig. 1a, we show the 4D phase space measured of the beam emitted from a large laser spot that covers multiple patterned markers on the cathode. Following the reconstruction theory, we obtain the 4D transfer matrix,

$$\mathbf{M} = \begin{pmatrix} -1.37(2) & -0.16(1) & -2.23(2) & 0.319(6) \\ -0.60(1) & -0.184(3) & -0.93(1) & -0.235(3) \\ -3.36(2) & -0.42(2) & 1.19(2) & 0.07(1) \\ -0.964(8) & -0.371(4) & 0.430(9) & 0.173(5) \end{pmatrix},$$

where the units of position and momentum are μm and keV/c, respectively. Using this transfer matrix and the 4D phase space in Fig. 1a, we reconstruct the source 4D phase space of the beam at the cathode, shown in Fig. 1b.

We analyze the reconstructed *x*-*y* position phase space in Fig. 2a, by taking linecut profiles across features induced by the substrate micro-pattern, shown in Fig. 2b. In the linecut profiles shown in Fig. 2c and Fig. 2d, the fiducial features appear as troughs in density, and we measure the center-to-center distances. Note that there is a background to the data in Fig. 2c due to the laser intensity varying spatially, and we take another linecut profile off the fiducial markers to estimate and subtract it from the data. The average center-to-center distance between features in the horizontal linecut shown in Fig. 2c is $102 \pm 4$ μm, which agrees with the spacing between the corresponding substrate fiducial markers, measured by a scanning electron microscope (SEM) in Fig. 2b to be 100 μm. We propagate the resolution of the aperture scan measurement to determine the uncertainties of the average center-to-center distances quoted here. The center-to-center distance between features in the vertical linecut profile shown in Fig. 2d is $207 \pm 5$ μm. This is slightly larger than the 200 μm spacing measured in the SEM image, but still within $2\sigma$. We also compare the MTE calculated from the reconstructed source momentum distribution to the MTE measured by an emittance measurement via the aperture scan. We measured 4D phase spaces for varying source beam sizes, $\sigma_x$, and reconstructed the source 4D phase spaces for each source beam size. Fitting each reconstructed source $p_x$-$p_y$ momentum phase space to a 2D supergaussian for $\langle p_x p_x \rangle_i$, $\langle p_y p_y \rangle_i$, and $\langle p_x p_y \rangle_i$, we use $\mathrm{MTE} = \sqrt{\langle p_x p_x \rangle_i \langle p_y p_y \rangle_i}/m_e$ to obtain the MTE of $73 \pm 2$ meV. Using a Monte Carlo simulation, we propagate the uncertainty of the measured partial transfer matrix to determine the uncertainty of the MTE. To confirm this MTE measurement, we calculated the 4D emittance, $\epsilon$, of each measured 4D phase space and linearly fitted it as a function of $\sigma_x$, $\epsilon = \sigma_x \sqrt{\mathrm{MTE}/m_e c^2}$, where $m_e$

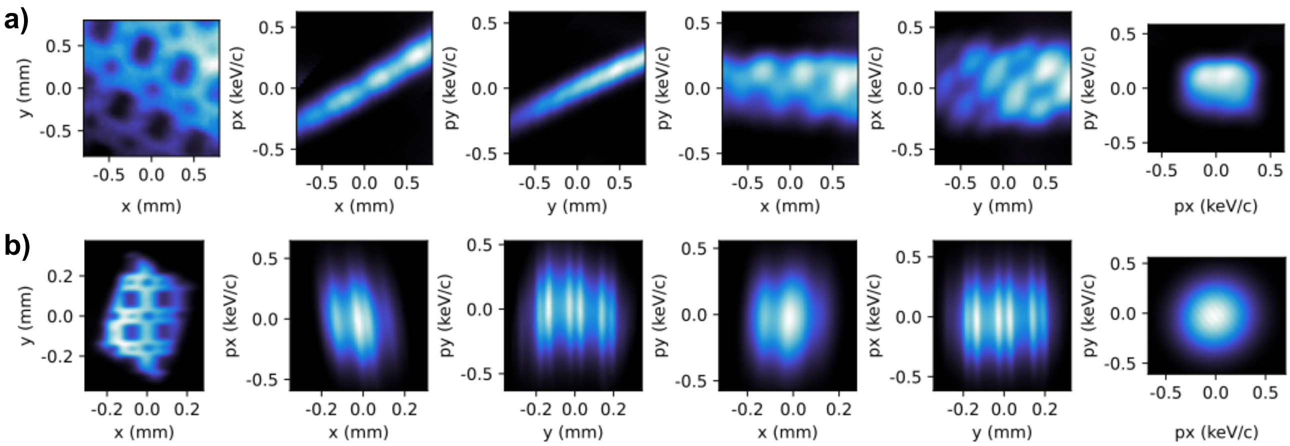


Figure 1: **a)** Measured 4D phase space of the beam at the aperture. Only a 1200 μm by 1200 μm part of the beam was measured. **b)** Reconstructed source 4D phase space of the beam at the cathode.

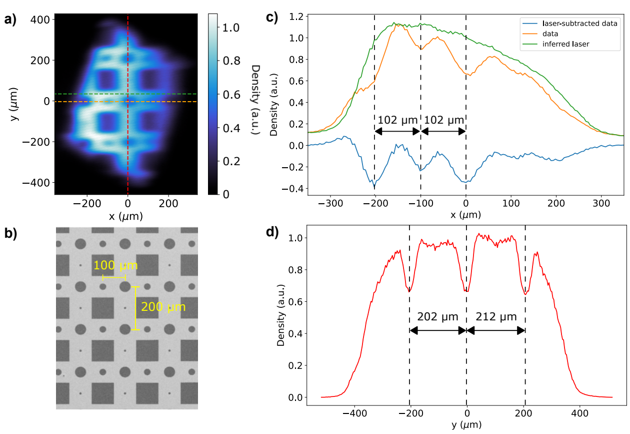


Figure 2: **a)** The reconstructed source *x*-*y* position phase space with linecut profiles taken along the dashed lines and correspondingly colored with the displayed curves in **c)** and **d)**. **b)** Scanning electron microscope image of the cathode substrate. Dark regions correspond to $SiO_2$, and copper for light regions. A Na-K-Sb thin film (not shown) is grown on top of the substrate. Black dashed lines in **c)** and **d)** indicate the center of fiducial features.

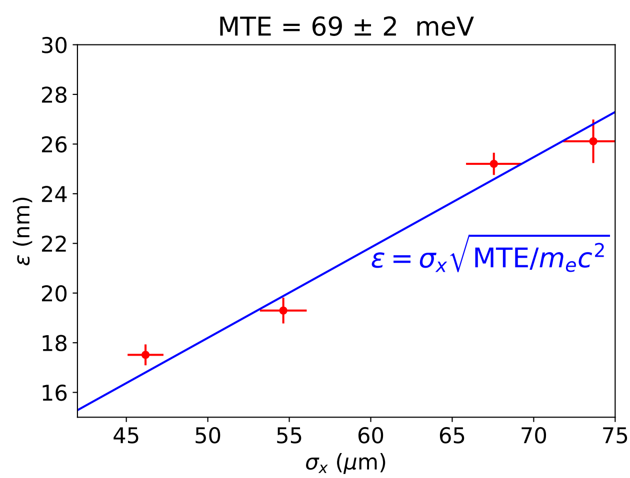


Figure 3: 4D emittance, $\epsilon$, measured as a function of beam size at the cathode, $\sigma_x$, and linearly fitted to yield an MTE of 69 $\pm$ 2 meV. The fit requires $\epsilon \to 0$ as $\sigma_x \to 0$.

is the electron mass. The data and the fit are shown in Fig. 3, yielding a MTE of 69 $\pm$ 2 meV. As such, we see that the MTE measured with the source phase space reconstruction and the emittance measurement agree, validating the source $p_x$-$p_y$ momentum phase space reconstruction.

## CONCLUSIONS

In this paper, we demonstrate a method for measuring the 4D transfer matrix between the source and a downstream aperture scan diagnostic by measuring the dependence of the 4D beam moments on the source emission position. In addition, we apply the measured transfer matrix to reconstruct the source 4D phase space of a beam emitted from a micro-patterned cathode. To verify the fidelity of the reconstruction, we analyzed the reconstructed source $p_x$-$p_y$ momentum phase space to directly determine the MTE and found that it agreed with aperture scan measurements of MTE. We also confirmed that the source *x*-*y* position phase space is reconstructed successfully by observing that the spacing between features in the reconstructed *x*-*y* position phase space matches that of the corresponding fiducial markers patterned onto the cathode. Altogether, this is suggestive that we are able to solve for the beam transfer matrix and apply it to reconstruct the source 4D phase space with good fidelity.

## ACKNOWLEDGMENTS


This work was supported by U.S. Department of Energy, Grants DE-SC0020144 and DE-AC02-76SF00515, and U.S. National Science Foundation Grant No. PHY-1549132, the Center for Bright Beams. Competing Interests: J.M. is a co-founder of Cayuga Beam Systems. The authors would also like to thank the CLASSE technical staff for their assistance with the building and maintenance of the PHOEBE test beamline and colleagues within the Center for Bright Beams for many insightful discussions.

# REFERENCES


[1] C. T. Parzyck *et al.*, "Single-crystal alkali antimonide photocathodes: high efficiency in the ultrathin limit", *Phys. Rev. Lett.*, vol. 128, no. 11, p. 114801, Mar. 2022. doi:10.1103/PhysRevLett.128.114801

[2] C. A. Pennington *et al.*, "A structural analysis of ordered cs3sb films grown on single crystal graphene and silicon carbide substrates", *APL Mater.*, vol. 13, no. 1, p. 011120, Jan. 2025. doi:10.1063/5.0229850

[3] S. Karkare *et al.*, "Ultracold electrons via near-threshold photoemission from single-crystal cu(100)", *Phys. Rev. Lett.*, vol. 125, no. 5, p. 054801, Jul. 2020. doi:10.1103/PhysRevLett.125.054801

[4] S. Karkare and I. Bazarov, "Effects of surface nonuniformities on the mean transverse energy from photocathodes", *Phys. Rev. Appl.*, vol. 4, no. 2, p. 024015, Aug. 2015. doi:10.1103/PhysRevApplied.4.024015

[5] G. S. Gevorkyan, S. Karkare, S. Emamian, I. V. Bazarov, and H. A. Padmore, "Effects of physical and chemical surface roughness on the brightness of electron beams from photocathodes", *Phys. Rev. Accel. Beams*, vol. 21, no. 9, p. 093401, Sep. 2018. doi:10.1103/PhysRevAccelBeams.21.093401

[6] M. Gordon *et al.*, "Four-dimensional emittance measurements of ultrafast electron diffraction optics corrected up to sextupole order", *Phys. Rev. Accel. Beams*, vol. 25, no. 8, p. 084001, Aug. 2022. doi:10.1103/PhysRevAccelBeams.25.084001